This advance publication article will be replaced by the finalized version after proofreading.

IEICE Communications Express, Vol.12, No.1, 1–4

ComEX

LETTER

Impact of base station density and altitude on transmission performance in millimeter-wave UAV communications

Shota Muroki[1], **Shuhei Saito**[1], **Hirofumi Suganuma**[1], **and Fumiaki Maehara**[1, a)]

Abstract A recent approach to expanding the coverage of 6G networks and enhancing disaster preparedness is the use of wireless networks based on unmanned aerial vehicles (UAVs), which can be positioned independent of ground conditions and provide line-of-sight communication with a high probability. In wireless communication using UAVs, propagation attenuation and interference vary significantly depending on UAV density and flight position. Therefore, understanding their quantitative effects on communication quality is crucial. Moreover, assuming the use of high-frequency bands, blockage also occurs; therefore, its impact must be evaluated. In this study, we evaluated the outage probability and throughput in millimeter-wave UAV wireless communication by varying UAV density and altitude using computer simulations. In particular, we clarify the effects of blockages specific to high-frequency bands on these performance criteria.

Keywords: unmanned aerial vehicle (UAV), millimeter-wave (mmWave), line-of-sight (LoS), outage probability, blockage

Classification: Wireless communication technologies

1. Introduction

In recent years, the demand for mobile services has continued to increase owing to the increase in digital content and rapid spread of Internet-of-things devices. The commercialization of the fifth-generation mobile communication system (5G) began in the spring of 2020 in Japan. This system includes enhanced mobile broadband (eMBB), which is an evolution of the fourth-generation mobile communication system (4G), ultra reliable and low latency communications (URLLC), and massive machine type communications (mMTC). Furthermore, considering the potential realization of the sixth-generation mobile communication system (6G) by 2030, area-traffic capacity is considered a crucial metric. The coverage area needs to be expanded to 1 Gbps/m^2, which is more than 100 times that of 5G [1]. In addition, in countries and regions, such as Japan, that are subject to various natural disasters such as earthquakes, tsunamis, and typhoons, the installation of emergency radio systems that can quickly restore networks, even if terrestrial radio equipment is damaged, is urgently needed [2]. In this context, the construction of wireless networks using unmanned aerial vehicles (UAVs) has garnered attention to achieve the envisioned coverage expansion and disaster countermeasures expected from 6G. Because UAVs can dynamically control their flight positions, UAVs equipped with wireless equipment, such as base stations (BSs), access points, and repeaters, can efficiently provide network connectivity to places that radio waves relying on ground-based wireless equipment cannot reach as well as disaster-stricken areas [2, 3].

In wireless communication using UAVs, the degree of propagation attenuation and interference changes significantly depending on the density and flight position of the UAVs; therefore, quantitatively understanding their effects on transmission performance is crucial. Reference [4] investigated the effect of UAV altitude on throughput performance based on wireless LAN standards. Reference [5] derived the effective deployment of a single UAV by considering the effect of human blockage owing to the use of millimeter-waves (mmWaves) in 5G networks. Reference [6] also assumed mmWaves and evaluated the coverage performance when considering the interference caused by multiple UAVs as well as a blockage. However, because this evaluation already considers the effects of a blockage, it is expected to elucidate the extent to which blocking, which is specific to high-frequency bands, affects performance.

In this study, we investigate the coverage performance and system capacity when the density and altitude of multiple UAVs are changed. This performance evaluation considers blockages particular to high-frequency bands and clarifies their effect on coverage performance and system capacity by comparing it with a case without the effect of blockages. Regarding the blockages, we apply a model in which pedestrians occur in a stationary Poisson process and change based on pedestrian density and speed, which is reflected in the received power of the mobile station (MS). This enables us to examine the effect of blockages on the performance of UAV wireless communications in high-frequency bands.

2. System model and analysis

Fig. 1 shows a wireless communication system using UAVs, where N_{U} and R are the number of UAV BSs and radius of communication area, respectively. As shown in the figure, multiple UAV BSs transmit radio waves from the sky, constructing a service area on the ground. Unlike BSs that are fixed on the ground, UAV BSs can flexibly change the conditions in their service areas by changing the altitudes and densities of the UAVs. However, because of the UAV altitude, if the MS is outside the service area, it may be out-of-service. In addition, in this study, we assume a high-frequency band, such as mmWaves, and consider the effect

[1] Graduate School of Fundamental Science and Engineering, Waseda University, 3-4-1 Ohkubo, Shinjuku-ku, Tokyo 169-8555, Japan

a) fumiaki_m@waseda.jp

©IEICE 2024
DOI: 10.23919/comex.2024XBL0075
Received March 31, 2024
Accepted April 09, 2024

This work is licensed under a Creative Commons Attribution NonCommercial, No Derivatives 4.0 License.
Copyright © 2023 The Institute of Electronics, Information and Communication Engineers

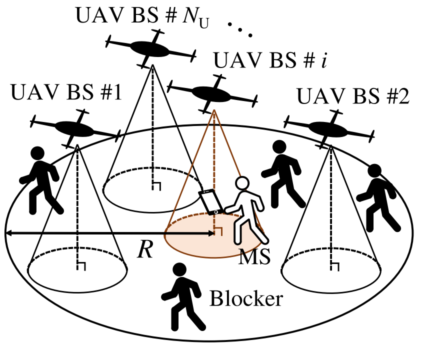

Fig. 1 Wireless communication system using UAVs.

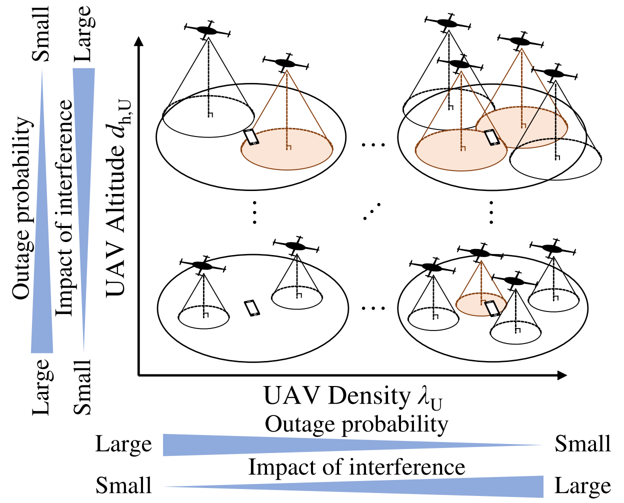

Fig. 2 Influence of UAV altitude and density on the transmission performance.

of blockages by pedestrians on the receiver. Therefore, even if the MS is within the service area, radio waves may not reach the area, resulting in the deterioration of the transmission performance.

Fig. 2 shows the influence of the UAV altitude and density on the transmission performance, assuming that multiple UAV BSs are uniformly distributed within a circular area centered on the desired MS and operate at the same altitude and frequency. Moreover, supposing that the number of UAV BSs N_{U} follows a Poisson distribution with the UAV density λ_{U}, its probability function can be given as $p(N_{\mathrm{U}}) = (\lambda_{\mathrm{U}}\pi R^2)^{N_{\mathrm{U}}} \exp(-\lambda_{\mathrm{U}}\pi R^2)/N_{\mathrm{U}}!$ [9]. As shown in the figure, increasing the UAV altitude $d_{\mathrm{h,U}}$ expands the coverage area and reduces its probability of being out-of-service; however, it is also strongly affected by interference from other UAV BSs. With respect to the UAV density, as the density λ_{U} increases, the coverage area of the UAV BS expands and the probability of the UAV BS being out-of-service decreases. However, the influence of interference from other UAV BSs increases. Therefore, the transmission performance of the MSs changes depending on the altitude and density of the UAVs, which must be clarified quantitatively.

Fig. 3 shows a scenario in which the MS is within or outside the coverage area in the presence of multiple UAV BSs. Here, each UAV BS is assumed to be able to tilt its antenna by the maximum angle $\phi_{\max}$ [7], and the coverage area C_i of the UAV BS #i can be determined from $\phi_{\max}$ and the UAV altitude. As shown in the figure, if a MS exists within the coverage area of any UAV BS, it is in service. However, if a MS exists outside the coverage area of all the UAV BSs, the MS is considered out-of-service. In this performance evaluation, each MS is assumed to select the UAV BS with the shortest link distance between the MS and UAV BS.

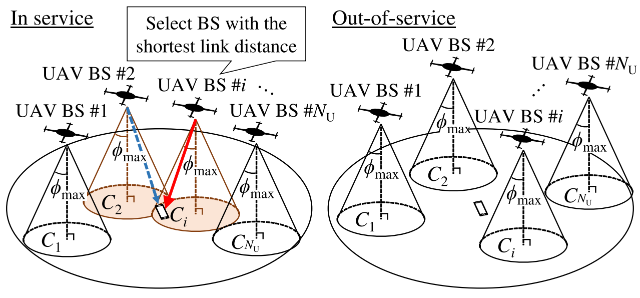

Fig. 3 A scenario in which the MS is within or outside the coverage area in the presence of multiple UAV BSs.

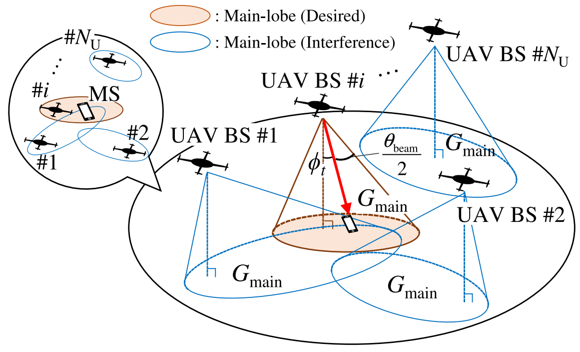

Fig. 4 Beamforming when each UAV BS and MS are connected.

Next, we explain the antenna directivity applied to each UAV BS, which is assumed in this study. Fig. 4 shows the beamforming when each UAV BS and MS are connected. The beamforming range is defined by the beamwidth θ_{beam} centered around the tilt angle ϕ_t, and antenna gain is assumed to be obtained when the MS is within the range of the main-lobe. Therefore, in this study, the side-lobe antenna gain is set to zero. Fig. 5 shows the antenna gain of the main-lobe [7, 8]. In addition, when the UAV BS is located at the origin, the range of the main-lobe area is an ellipse with center $(r_e, 0)$, major axis r_M, and minor axis r_m, as given by [7]:

$$r_M = \frac{(d_{\mathrm{h,U}} - d_{\mathrm{h,M}}) \sin(\theta_{\mathrm{beam}})}{2\left(\cos^2(\phi_t) - \sin^2(\theta_{\mathrm{beam}}/2)\right)}, \tag{1}$$

$$r_m = \frac{(d_{\mathrm{h,U}} - d_{\mathrm{h,M}}) \sin(\theta_{\mathrm{beam}}/2)}{\sqrt{\cos^2(\phi_t) - \sin^2(\theta_{\mathrm{beam}}/2)}}, \tag{2}$$

$$r_e = (d_{\mathrm{h,U}} - d_{\mathrm{h,M}}) \tan(\phi_t - \theta_{\mathrm{beam}}/2) + r_M. \tag{3}$$

Furthermore, we assume that UAV BSs other than the desired UAV BS of interest would always communicate with any MS. Therefore, as shown in the figure, if the desired MS is within the main-lobe range of another UAV BS, interference occurs, and the transmission performance deteriorates.

Moreover, in addition to the antenna directivity, we consider the impact of blockages owing to the use of high-

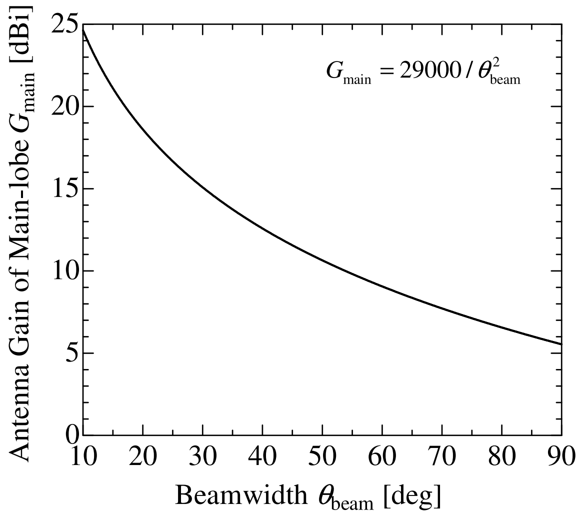

Fig. 5 Antenna gain of the main-lobe.

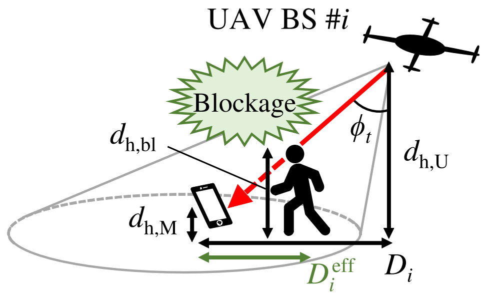

Fig. 6 Receiving condition of the MS in the presence of a blockage caused by mobile blockers.

frequency bands, such as mmWaves, in our performance evaluation. Fig. 6 shows the receiving condition of the MS in the presence of a blockage caused by mobile blockers. Assuming that the blockage occurs based on a stationary Poisson process, its probability function employing the antenna height and user-position information can be given as follows [9]:

$$P = \frac{(2/\pi)\lambda_{bl} D_i^{eff} V}{\mu + (2/\pi)\lambda_{bl} D_i^{eff} V}, \tag{4}$$

$$D_i^{eff} = \frac{d_{h,bl} - d_{h,M}}{d_{h,U} - d_{h,M}} \cdot D_i, \tag{5}$$

where $1/\mu$ is the expected blockage duration; λ_{bl} and V are the density and velocity of the blockers, respectively; $d_{h,bl}$ and $d_{h,M}$ are the heights of blockers and MS, respectively; D_i is the link distance between UAV BS #i and MS; and D_i^{eff} is the effective link distance between UAV BS #i and MS, which indicates the distance affected by the movement of the blocker. In this scenario, the throughput when UAV BS #i is selected, considering the interference between UAV BSs, can be calculated as follows [10]:

$$S_i = B \log_2 \left(1 + \frac{W_i |h_i|^2 G_M G_{U,i} P_x}{\left(\sum_{k=1,k\neq i}^{N_U} W_k |h_k|^2 G_M G_{U,k} P_x \right) + P_n} \right), \tag{6}$$

Table I System Parameters

Carrier frequency f_c / Bandwidth B	28 GHz / 1 GHz
Radius of communication area	100 m
Transmit power of UAV BS P_x	20 dBm
Channel model	AWGN
UAV altitude $d_{h,U}$	10 ~ 100 m
Height of MS antenna $d_{h,M}$	1.5 m
Height of blocker $d_{h,bl}$	1.8 m
Velocity of blocker V	3.0 km/h
Density of blockers λ_{bl}	0.9 bl/m^2
Expected blockage duration $1/\mu$	0.5 s
Beamwidth of UAV antenna θ_{beam}	60 deg
Maximum tilt angle of UAV antenna ϕ_{max}	30 deg
UAV antenna gain of main-lobe [7, 8]	$29000/\theta_{beam}^2$
MS antenna gain	0 dBi
Thermal noise density	−174 dBm/Hz
Noise figure	10 dB

where B is the bandwidth; $G_{U,i}$ and G_M are the antenna gains of UAV BS #i and MS; P_x and P_n are transmit and noise power; h_i is the channel condition between UAV BS #i and MS; W_i is a coefficient that takes the value 0 when the blockage occurs or 1 otherwise. Regarding the channel model, the direct wave without fading is considered, and its propagation loss is expressed as follows [6, 11]:

$$L_i = \left(\frac{4\pi}{\lambda}\right)^2 \left(D_i^2 + \left(d_{h,U} - d_{h,M}\right)^2\right)^{\alpha_L/2}, \tag{7}$$

where λ is the wavelength and α_L is the path-loss exponent that takes a value of 2 in the case of carrier frequency f_c = 28 GHz.

3. Numerical results

In this section, we evaluate the effects of UAV altitude and density on the outage probability and throughput in UAV wireless communication using high-frequency bands. We also examine the effects of blocking on these parameters. Table I shows the simulation parameters used in this study. In this evaluation, the UAV BSs are assumed to be uniformly distributed at the same altitude within a circular area centered on the desired MS. In addition, the UAV density varies between 100 and 1000/km^2, and the blocker parameters, such as height $d_{h,bl}$, density λ_{bl}, and velocity V, are set based on the ITU-R report [12].

Fig. 7 shows the outage probability versus the altitude $d_{h,U}$ of the UAV BS considering the presence or absence of blockages. The figure shows that regardless of the density of the UAV BSs, as the altitude of the UAV BSs increase, the service area of each BS expands and the outage probability decreases. Moreover, as the density of the UAV BSs increases, the number of BSs existing in a cell increases, and the service area expands; thus, the outage probability decreases. Furthermore, a comparison of the cases with and without blockages shows that the outage probability increases when including the effect of blockages. This is because blockages narrow the service area.

Fig. 8 shows the throughput performance versus altitude $d_{h,U}$ of the UAV BS with and without blockages. The figure shows that when the BS density λ_{BS} = 100/km^2, increasing

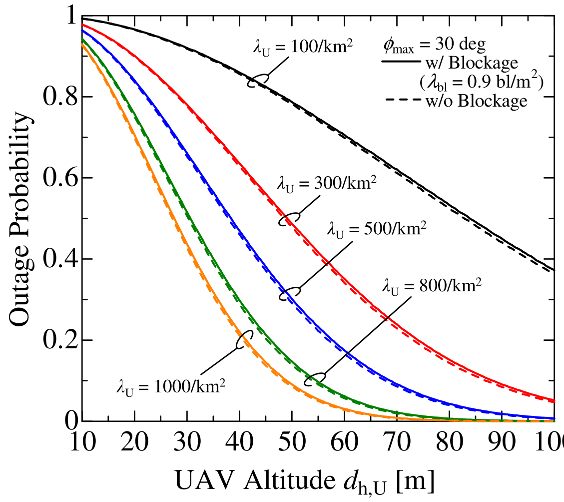

Fig. 7 Outage probability versus UAV altitude $d_{h,U}$.

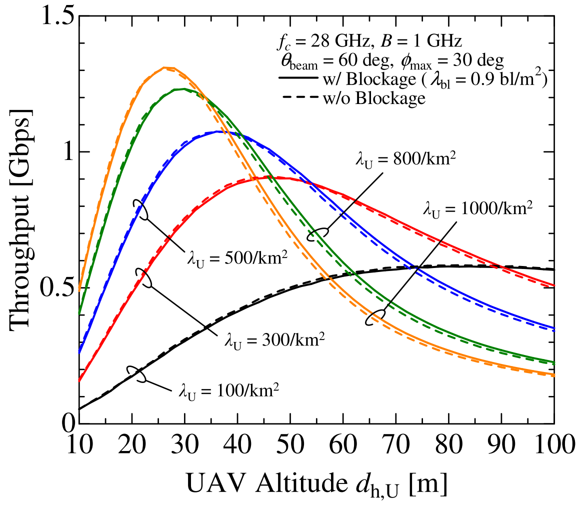

Fig. 8 Throughput versus UAV altitude $d_{h,U}$.

the altitude of the UAV BS reduces the outage probability and improves throughput. However, when the BS density exceeds $300/\text{km}^2$, the throughput improves up to a particular altitude and then begins to decrease. This is because as the density of UAV BSs increases, the interference between UAV BSs is exacerbated, which reduces the throughput, especially at high UAV altitudes. Furthermore, when comparing the cases with and without blockages, at a low UAV altitude, the throughput with a blockage is lower than that without a blockage. However, at a high UAV altitude, the throughput when considering a blockage is higher than that without considering a blockage. Therefore, when the UAV BS is at a low altitude, throughput decreases owing to the received signal-power reduction due to a blockage. However, when the UAV altitude increases, the blockage contributes to reducing the interference between UAV BSs, which leads to enhanced SINR. Therefore, at high UAV altitudes, blockages can improve the throughput of UAV wireless communications.

4. Conclusion

In this study, we investigated the coverage performance and system capacity of UAV wireless communications using mmWaves via computer simulations. In particular, we clarified the effects of blockages by pedestrians, specific to high-frequency bands, on transmission performance as well as the effects of changes in the density and altitude of multiple UAVs. The performance evaluation revealed that as the altitude and density of the UAV BSs increased, the service area expanded, and the outage probability decreased. Moreover, blockages specific to mmWaves increased the outage probability, regardless of the UAV density and altitude. As the UAV altitude increased, the throughput improved owing to a decrease in outage probability. However, from a particular UAV altitude, the interference between UAV BSs intensified, which decreased the throughput. Interestingly, blockages contribute to improving throughput by reducing interference from other UAV BSs at a high UAV altitude, whereas blockages only reduce throughput owing to the received signal-power reduction at a low UAV altitude.

In our future investigations, we will assess the impact of various blockers, such as trees or buildings other than pedestrians, on mmWave UAV communications.

References

[1] Z. Zhang, Y. Xiao, Z. Ma, M. Xiao, Z. Ding, X. Lei, G. K. Karagiannidis, and P. Fan, "6G wireless networks: Vision, requirements, architecture, and key technologies," *IEEE Veh. Technol. Mag.*, vol. 14, no. 3, pp. 28–41, Sept. 2019.

[2] M. Mozaffari, W. Saad, M. Bennis, Y.-H. Nam, and M. Debbah, "A tutorial on UAVs for wireless networks: Applications, challenges, and open problems," *IEEE Communications Surv. & Tut.*, vol. 21, no. 3, pp. 2334–2360, May 2019.

[3] M. A. Khan, N. Kumar, S. A. H. Mohsan, W. U. Khan, M. M. Nasralla, M. H. Alsharif, J. Żywiołek, and I. Ullah, "Swarm of UAVs for network management in 6G: A technical review," *IEEE Trans. Netw. Service Manage.*, vol. 20, no. 1, pp. 741–761, Mar. 2023.

[4] M. Ishigami and T. Sugiyama, "A novel drone's height control algorithm for throughput optimization in disaster resilient network," *IEEE Trans. Veh. Technol.*, vol. 69, no. 12, pp. 16188–16190, Dec. 2020.

[5] M. Gapeyenko, I. Bor-Yaliniz, S. Andreev, H. Yanikomeroglu, and Y. Koucheryavy, "Effects of blockage in deploying mmWave drone base stations for 5G networks and beyond," Proc. 2018 IEEE Int. Conf. Commun. Workshops (ICC Workshops 2018), pp. 1–6, May 2018.

[6] W. Yi, Y. Liu, Y. Deng, A. Nallanathan, "Clustered UAV networks with millimeter wave communications: A stochastic geometry view," *IEEE Trans. Commun.*, vol. 68, no. 7, pp. 4342–4357, July 2020.

[7] M. M. Azari, F. Rosas, and S. Pollin, "Cellular connectivity for UAVs: Network modeling, performance analysis, and design guidelines," *IEEE Trans. Wireless Commun.*, vol. 18, no. 7, pp. 3366–3381, July 2019.

[8] C. A. Balanis, *Antenna Theory: Analysis and Design*, Hoboken, NJ, USA: Wiley, 2016.

[9] I. K. Jain, R. Kumar, and S. S. Panwar, "The impact of mobile blockers on millimeter wave cellular systems," *IEEE J. Sel. Areas Commun.*, vol. 37, no. 4, pp. 854–868, April 2019.

[10] G. Hosoi, M. Nitta, S. Saito, H. Suganuma, and F. Maehara, "Impact of antenna directivity on blockage mitigation method employing antenna height and user position in millimeter-wave communications," *IEICE Commun. Express*, vol. 12, No. 3, pp. 96–101, Mar. 2023.

[11] T. S. Rappaport, E. B-Dor, J. N. Murdock, and Y. Qiao, "38 GHz and 60 GHz angle-dependent propagation for cellular & peer-to-peer wireless communications," Proc. 2012 IEEE Int. Conf. Commun. (ICC 2012), pp. 4568–4573, June 2012.

[12] Report ITU-R M.2412-0, "Guidelines for evaluation of radio interface technologies for IMT-2020," Oct. 2017.